https://doi.org/10.5194/bg-2020-409
Preprint. Discussion started: 11 November 2020

Biogeosciences
Discussions
Open Access
EGU

Quantifying the Importance of Antecedent Fuel-Related Vegetation Properties for Burnt Area using Random Forests

Alexander Kuhn-Régnier[1,2], Apostolos Voulgarakis[1,2,3], Peer Nowack[2,4,5], Matthias Forkel[6], I. Colin Prentice[1,7], and Sandy P. Harrison[1,8]

[1]Leverhulme Centre for Wildfires, Environment, and Society
[2]Department of Physics, Imperial College London, UK
[3]School of Environmental Engineering, Technical University of Crete, Chania, Greece
[4]Grantham Institute and the Data Science Institute, Imperial College London, UK
[5]Climatic Research Unit, School of Environmental Sciences, University of East Anglia, UK
[6]Environmental Remote Sensing Group, TU Dresden, Dresden, Germany
[7]Department of Life Sciences, Imperial College London, UK
[8]Geography and Environmental Science, University of Reading, UK

Correspondence: Alexander Kuhn-Régnier (alexander.kuhn-regnier14@imperial.ac.uk)

https://doi.org/10.5194/bg-2020-409
Preprint. Discussion started: 11 November 2020

Biogeosciences Discussions

Abstract. The seasonal and longer-term dynamics of fuel accumulation affect fire seasonality and the occurrence of extreme wildfires. Failure to account for their influence may help to explain why state-of-the-art fire models do not simulate the length and timing of the fire season or interannual variability in burnt area well. We investigated the impact of accounting for different timescales of fuel production and accumulation on burnt area using a suite of random forest regression models that included the immediate impact of climate, vegetation, and human influences in a given month, and tested the impact of various combinations of antecedent conditions in four productivity-related vegetation indices and in antecedent moisture conditions. Analyses were conducted for the period from 2010 to 2015 inclusive. We showed that the inclusion of antecedent vegetation conditions on timescales > 1 yr had no impact on burnt area, but inclusion of antecedent vegetation conditions representing fuel build-up led to an improvement of the global, climatological out-of-sample R^2 from 0.567 to 0.686. The inclusion of antecedent moisture conditions also improved the simulation of burnt area through its influence on fuel build-up, which is additional to the influence of current moisture levels on fuel drying. The length of the period which needs to be considered to account for fuel build-up varies across biomes; fuel-limited regions are sensitive to antecedent conditions over longer time periods ($\sim$4 months) and moisture-limited regions are more sensitive to current conditions.

1 Introduction

Wildfires are an important natural disturbance of the Earth System. They have extensive socio-economic impacts as well as profound effects on vegetation, atmospheric composition, and climate (Bowman et al., 2011; Voulgarakis and Field, 2015; Andela et al., 2017; Lasslop et al., 2019). How fire regimes may change in the future, and how fire-related feedbacks may influence climate and global environmental changes are growing concerns.

The factors that influence the occurrence and intensity of fire are well-known: the presence of an ignition source, vegetation properties that determine the availability of fuel, and weather conditions that promote fuel drying and thereby the rate of fire spread. Human activities are also implicated, either promoting or suppressing fire through ignitions, fuel management, and landscape modification. However, these factors are strongly coupled to one another. Climate conditions influence the incidence of lightning and the nature of the vegetation, while wind strength and the impact of atmospheric conditions on drying are modulated by vegetation cover. Furthermore, the relationships among ignitions, vegetation, and climate may depend on the timescales involved. Short-term drought promotes fuel drying and hence increases the risk of fire, but in the longer term, drought conditions reduce vegetation cover and fuel loads. This complexity makes it challenging to disentangle the causes of observed changes in fire regimes. Recent declines in burnt area (BA) in some regions have been explained as a consequence of human activity, through indirect and direct intervention (Martínez et al., 2009; Andela et al., 2017) albeit modulated by climate and vegetation (Forkel et al., 2019b). However, it has been argued that climate may become increasingly important in the future (Pechony and Shindell, 2010; Abatzoglou and Williams, 2016; Bowman et al., 2017; Barbero et al., 2015; Goss et al., 2020), especially in the extratropics (Yang et al., 2014). Indeed, a mainly temperature-driven increase in conditions conducive to wildfires was suggested by a number of regional studies (e.g. Westerling, 2006; van Oldenborgh et al., 2020; Goss et al.,

https://doi.org/10.5194/bg-2020-409
Preprint. Discussion started: 11 November 2020

2020; Barbero et al., 2015). At the global scale, Abatzoglou et al. (2019) showed that anthropogenic climate change had led to an increase in fire weather over 22% of the global burnable area by 2019, while Jolly et al. (2015) found that anthropogenic climate change has led to a lengthening of the fire season across more than a quarter of global vegetated land in recent decades. Increases in fire weather are predicted under different assumptions about levels of future warming (e.g. Burton et al., 2018; Turco et al., 2018; Bedia et al., 2015).

Understanding the interplay among the different present-day controls of fire is also a key requirement for the prediction of future fire-regime shifts and impacts on the land biosphere and human activities. Coupled fire-vegetation models can be used to predict changes in large-scale fire regimes in response to future climate change scenarios (see e.g. Knorr et al., 2016; Kloster et al., 2012) and to explore how these changes are affected by and will affect regional vegetation patterns and climate. Although these models are reasonably good at simulating modern geographical fire patterns in BA, they are poor at reproducing observed fire-season length and inter-annual variability (IAV) in BA (Hantson et al., 2020). Furthermore, there are large differences in their predictions of both historical (Teckentrup et al., 2019) and future (Kloster and Lasslop, 2017; Sanderson and Fisher, 2020) trends.

Studies have pinpointed the relationship between simulated vegetation properties and BA as a cause for concern (e.g. Forkel et al., 2019a; Kelley et al., 2019; Teckentrup et al., 2019; Hantson et al., 2020). Forkel et al. (2019a) analysed satellite data to show that while state-of-the-art fire–vegetation models reproduce the emergent relationships with climatic variables, they do not correctly represent the relationship between vegetation and BA. Hantson et al. (2020) highlighted the need for improved understanding of vegetation drivers of fire season length and inter-annual variability (IAV) of BA. Both Forkel et al. (2019a) and Hantson et al. (2020) argued for a better understanding of how vegetation properties control fuel build-up, and therefore fire occurrence and intensity.

Fuel is organic matter that is available for ignition (Keane et al., 2001). The type, amount, and spatial arrangement of fuel affect its tendency to burn (Archibald et al., 2009). These properties, dictated by vegetation, in turn affect fuel connectivity and hence fire spread in addition to how rapidly fuel dries out and becomes combustible. The accumulation of fuel over time is expected to influence fire intensity. Antecedent weather conditions in the weeks to years before fire events can also determine fuel availability (van Oldenborgh et al., 2020) and hence fire occurrence. The effect of antecedent weather conditions on BA may depend on the types of vegetation present: antecedent precipitation will increase BA in fuel-limited regions, for example, but decrease BA in regions where fuel drying is the major control (Alvarado et al., 2020; Abatzoglou and Kolden, 2013). A better understanding of the timescales of fuel accumulation, the interaction between biophysical drivers and fuel build-up, and the effects of antecedent weather conditions on both fuel loads and fuel drying is needed in order to improve predictions of BA.

In this study, we investigate the importance of current and antecedent conditions on BA, focusing particularly on the link of BA to antecedent vegetation productivity and aridity. Since other climate factors, ignitions, and human activities also influence BA, we necessarily include these factors in our analysis. We use a machine learning approach to identify non-linear relationships and interactions between the drivers. This is supported by analysis and visualisation techniques designed to mitigate the effects of correlations among variables, and to provide insights into the modelled interactions.

https://doi.org/10.5194/bg-2020-409
Preprint. Discussion started: 11 November 2020


Biogeosciences Discussions

2 Methods

2.1 Data

The predictor and BA datasets are available for different but overlapping time periods (Table 1). We pre-processed each dataset separately and conducted random forest analyses based on the common period from January 2010 to April 2015. Monthly fractional BA for this period was obtained from the GFED4 dataset (Giglio et al., 2013) (data were retrieved from https://www.globalfiredata.org/data.html).

Diurnal temperature range (DTR), maximum temperature (MaxT), dry-day period (DD), and soil moisture are important climate factors influencing BA (Archibald et al., 2009; Bistinas et al., 2014; Forkel et al., 2017, 2019a; Abatzoglou et al., 2018; Kelley et al., 2019) and are thus considered as predictors in our analyses. DTR was calculated by taking the monthly average of the difference between the daily maximum and minimum ERA5 (Copernicus Climate Change Service (C3S), 2017) 2 m temperatures. The dry-day period was defined as the longest contiguous period of ERA5 mean daily precipitation below 0.1 mm day^{-1} (wetting rainfall; Harris et al., 2014; Jolly et al., 2015) within each month. If this period was contiguous with a preceding dry-day period, these were concatenated. Soil moisture was taken from the Copernicus soil water index (SWI) dataset (Albergel et al., 2008; Wagner et al., 1999). We used the World Wide Lightning Location Network (WWLLN) dataset (Kaplan and Lau, 2019) which provides counts of monthly lightning ground strikes.

Land cover was shown in previous studies to be another important influence on BA. We included several alternative representations of land cover including above-ground tree biomass (AGB) and the fractional cover of trees (TREE), shrubs (SHRUB), herbaceous vegetation (HERB), and crops (CROP) in our predictor set. Tree AGB was obtained by combining AGB datasets for the tropics and for northern forests (Avitabile et al., 2016; Thurner et al., 2014). Yearly land cover values were obtained from the ESA CCI Land Cover dataset (Li et al., 2018). Land cover types were converted to fractional cover according to Poulter et al. (2015) using the conversion table as in Forkel et al. (2017). Global population density (POPD) from the HYDE 3.2 dataset (Klein Goldewijk, 2017) was used as a measure of human influence on vegetation and fire regimes.

Field data on fuel loads is sparse and the only global dataset (Pettinari and Chuvieco, 2016) is based on extrapolating scattered field measurements by biome. We therefore used four remotely sensed vegetation properties related to total biomass or leaf cover that could be regarded as indices for fuel load in our predictor set: solar-induced fluorescence (SIF), vegetation optical depth (VOD), fraction of absorbed photosynthetically active radiation (FAPAR), and leaf area index (LAI). All four properties have previously been used as productivity indices (e.g. Mohammed et al., 2019; Ryu et al., 2019; Teubner et al., 2018; Ogutu et al., 2014) and we use all four because it is uncertain which would be most closely related to fuel loads. Monthly SIF was obtained from the GlobFluo SIF dataset (Köhler et al., 2015). Ku-band VOD was obtained from the VODCA dataset (Moesinger et al., 2020). FAPAR and LAI were obtained from the MOD15A2H dataset (Myneni et al., 2015). For pre-processing, we used data from January 2008 to April 2015 for which period all four datasets are available.

https://doi.org/10.5194/bg-2020-409
Preprint. Discussion started: 11 November 2020

Biogeosciences Discussions Open Access EGU

Table 1. Characteristics of the datasets.

Variable	Abbreviation	Dataset	Start	End	Time	Reference
burnt area	BA	GFED4	06-1995	12-2016	monthly	Giglio et al. (2013)
diurnal temperature range, maximum temperature, dry-day period	DTR, MaxT, DD	ERA5	01-1990	12-2018	monthly	Copernicus Climate Change Service (C3S) (2017)
soil moisture	SWI	Copernicus SWI	01-2007	11-2018	monthly	Albergel et al. (2008); Wagner et al. (1999)
lightning	Lightning	WWLLN Lightning	01-2010	12-2018	monthly	Kaplan and Lau (2019)
above-ground tree biomass	AGB	Tropical AGB: Avitabile, Northern AGB: Thurner	static	static	static	Avitabile et al. (2016); Thurner et al. (2014)
land cover (fractional cover per grid cell)	CROP, SHRUB, TREE, HERB	ESA CCI Land Cover	1992	2015	yearly	Li et al. (2018)
solar-induced fluorescence	SIF	GlobFluo SIF	01-2007	04-2015	monthly	Köhler et al. (2015)
vegetation optical depth	VOD	VODCA (Ku-band)	12-1997	12-2018	monthly	Moesinger et al. (2019)
fraction of absorbed photosynthetically active radiation, leaf area index	FAPAR, LAI	MOD15A2H	02-2000	11-2018	monthly	Myneni et al. (2015)
population density	POPD	HYDE 3.2	2000	2017	yearly	Klein Goldewijk (2017)

2.2 Data processing

There are gaps in the SWI, FAPAR, LAI, SIF, and VOD datasets in winter months at latitudes above $\sim 60°$N, and in the austral winter for southern South America, due to high sun zenith angles for FAPAR, LAI, and SIF and because of snow cover and frozen soil for SWI and VOD (e.g. Moesinger et al., 2020). There are also sporadic missing values in these datasets caused by e.g. cloud cover. Missing values affect the calculation of antecedent conditions. These gaps were therefore filled using a two-step approach as in Forkel et al. (2017) for each location. First, persistent gaps, defined as months for which 50% or more of the observations across all years are missing, were filled using the minimum value observed at that location, for the given predictor variable. Second, transient gaps were filled using a season-trend regression model with four harmonic terms (k=4) and without breakpoints. These models were fitted using ordinary least square regression to the entire timeseries obtained during the first step, as mentioned before using data from January 2008 to April 2015. Locations where no observations were available for > 52 months out of the total 88 months were discarded in a trade-off between data quality and geographic extent. Missing land cover data, which mostly occurred in fire-free regions, were replaced by global minimum area fractions: (HERB:6.171491×10^{-6}; CROP: 4.936834×10^{-5}).

All datasets were interpolated to a common $0.25°$ spatial grid. Datasets where the original spatial resolution was higher than this were averaged; the other datasets were interpolated using nearest-neighbour interpolation to avoid smoothing local extrema (Forkel et al., 2017). Datasets that were only available at yearly time resolution (i.e. land cover, POPD) were linearly

https://doi.org/10.5194/bg-2020-409
Preprint. Discussion started: 11 November 2020


Biogeosciences Discussions Open Access EGU

interpolated to monthly intervals. Temporally static data (i.e. AGB) were recycled. Processing was carried out before averaging to provide monthly climatological time series.

The influence of antecedent conditions that might affect fuel loads or fuel dryness, specifically vegetation properties and DD, on BA was investigated by using antecedent FAPAR, LAI, VOD, SIF, and DD data from up to two years before any given month (1M, 3M, 6M, 9M, 12M, 18M, 24M, where M denotes months). The large autocorrelation between predictor variables could impede the interpretation of the impacts of antecedent periods ≥ 1 yr. Thus, anomalies were computed by subtracting the seasonal cycle relative to the designated month, resulting in the following transformations:

$$(\mathrm{X\ 12M}) - \mathrm{X} \rightarrow \mathrm{X}\ \Delta 12\mathrm{M},$$
$$(\mathrm{X\ 18M}) - (\mathrm{X\ 6M}) \rightarrow \mathrm{X}\ \Delta 18\mathrm{M},$$
$$\text{and } (\mathrm{X\ 24M}) - \mathrm{X} \rightarrow \mathrm{X}\ \Delta 24\mathrm{M},$$

where $\mathrm{X} \in \{\text{FAPAR, LAI, VOD, SIF, DD}\}$.

2.3 Machine learning experiments

We used random forest (RF) regression to model the relationships between BA and the driver variables (predictors). RF is an ensemble learning approach in which multiple decision trees are constructed using a randomly sampled subset of training observations. The final model is the average result from all of the individual decision trees. RF regression is highly suited to investigating the emergent controls on fire because it is able to learn non-linear relationships in high-dimensional space (Archibald et al., 2009). By averaging over multiple decision trees, RFs also mitigate overfitting (Breiman, 2001). We used the scikit-learn version 0.23.0 (Pedregosa et al., 2011) RF regression implementation in Python, with hyperparameters determined using five-fold cross validation of the final model: `n_estimators`: 500, `max_depth`: 18, `min_samples_leaf`: 3, `ccp_alpha`: 2×10^{-9}, and default values for all other parameters. The number of estimators (`n_estimators`) determines the number of trees whose predictions are averaged. The maximum depth (`max_depth`) limits the number of split levels. Setting `min_samples_leaf` to three requires that all final splits contain at least three samples. Finally, the `ccp_alpha` parameter controls the cost-complexity pruning algorithm that penalises a large number of splits if this does not increase performance sufficiently. By limiting the number of splits according to different metrics, these measures reduce overfitting. The validation dataset was randomly sampled across space and time and comprised 30% of the data. The gap between the R^2 values obtained on the training and validation datasets provides a measure of the generalisability of a given model, where a reduction in the training–validation gap indicates a greater capacity to identify underlying relationships accurately.

We trained a number of different RF regression models to test explicit hypotheses about the importance of antecedent conditions on BA (see Table 2) using the defined hyperparameters on the climatological timeseries. The initial experiment (ALL) was run using the basic set of 15 predictor variables related to climate, vegetation, and human influences on fire (Table 1) and included both current and antecedent values of the four vegetation indices and DD, giving 50 predictor variables. A second experiment (TOP15) used only the 15 most important predictors from the ALL model, as a way of testing whether all the predictors were necessary and whether including so many predictors resulted in overfitting. All of the remaining experiments used

https://doi.org/10.5194/bg-2020-409
Preprint. Discussion started: 11 November 2020


Biogeosciences Discussions Open Access EGU

Table 2. The modelling experiments. Except for the ALL experiment, the other experiments included 15 predictor variables for comparability. Differences in number of antecedent variables included in each experiment meant that different numbers of variables from the basic set were used in these experiments. For the TOP15, 15VEG_X, and BEST15 models we used the most important variables from the ALL experiment up to the required number of 15. For the CURRDD_X models, we used the most important variables from the CURR model. Table S1 provides a detailed list of the variables included in each experiment.

Name	Nr.	Variables
ALL	50	Basic set of current variables + current month and antecedent (1, 3, 6, 12, 18, 24M) values for Dry Days and vegetation indices (FAPAR, LAI, VOD, SIF)
TOP15	15	Top 15 predictors from the ALL model
CURR	15	Only current values of the basic set of 15 variables
15VEG_X (e.g. 15VEG_FAPAR)	15	Top 10 non-vegetation variables from the ALL experiment, plus current and antecedent (1, 3, 6, 9 months) vegetation index X (e.g. FAPAR)
CURRDD_X (e.g. CURRDD_FAPAR)	15	Current and antecedent (1, 3, 6, 9 months) versions of the vegetation index X (e.g. FAPAR), current DD, top 9 other variables from the CURR experiment
BEST15	15	Current and antecedent DD, one current, 1M, 3M, 6M, 9M vegetation index (drawn from the four potential vegetation indices) and 5 most important other variables from the basic set.

combinations of 15 predictor variables. The CURR experiment only used current-month values of each predictor. Comparison of the CURR, ALL, and TOP15 experiments allowed the impact of including antecedent vegetation and moisture conditions to be evaluated. Some of the vegetation predictors are highly correlated with one another and this could artificially decrease their importance in the ALL model. To test this, we ran four further experiments (15VEG_FAPAR, 15VEG_LAI, 15VEG_VOD, 15VEG_SIF) that included the 10 most important non-vegetation predictors from the ALL model. In addition, each of these experiments contained one of the four vegetation predictors represented by both current and antecedent values for 1M, 3M, 6M, and 9M. These four experiments all included current and antecedent values of DD. To separate out the effects of antecedent DD and antecedent vegetation properties, we ran a second set of vegetation experiments (CURRDD_FAPAR, CURRDD_LAI, CURRDD_VOD, CURRDD_SIF) where each vegetation predictor was represented by both current and antecedent values for 1M, 3M, 6M, and 9M but only using current DD and the next nine most important other factors from the CURR model. Finally, five-fold cross validation was used to isolate the best combination of the vegetation predictors under the constraint that each of the four antecedent states (1M–9M) must be represented exactly once (using any of the vegetation predictors), resulting in the BEST15 model.

2.4 Measuring predictor importance and relationships

Our goal is to determine the contribution of individual predictors (including antecedent states of these predictors) to model skill at predicting BA, and to examine the relationships between predictors and BA.

There is no unique way to measure the importance of a given predictor on model skill in predicting BA and it is particularly difficult to assign importance to individual predictors when there is a high degree of collinearity between them (Dormann et al.,

https://doi.org/10.5194/bg-2020-409
Preprint. Discussion started: 11 November 2020


Biogeosciences Discussions Open Access EGU

2013; Nowack et al., 2018; Mansfield et al., 2020). We use four techniques to assess the robustness of the inferred importance of individual predictors: Gini impurity, permutation feature importance (PFI), leave-one-column-out (LOCO), and SHapley Additive exPlanations (SHAP) values. The Gini importance aggregates the decrease in mean squared error (MSE) for each split involving a given predictor variable over the individual decision trees making up the RF. The PFI was calculated from five permutations of each predictor variable using ELI5 0.10.1 PermutationImportance (https://eli5.readthedocs.io/en/latest/index.html). While this provides an alternative assessment of the prediction score, the permutations may result in unlikely or impossible combinations of predictors and thus the PFI approach has a known tendency to overemphasise the importance of individual variables (Hooker and Mentch, 2019). The LOCO importance measure is estimated by repeatedly retraining the RF models, each time without one particular predictor variable. The relative importance of this predictor variable is then measured as the change in MSE on the training dataset, where a larger drop in MSE signifies a larger significance for the variable within the dataset. The importance of correlated predictor variables may be under-emphasised in this approach since the model is retrained. The SHAP value (Lundberg and Lee, 2017; Lundberg et al., 2020) is the average of the marginal contributions from a series of perturbations of the predictor variables. In a similar way to the PFI, this method shares the importance amongst correlated predictor variables, which may make them appear less significant than if they were included on their own. As for the other metrics, SHAP values were computed on all training samples. However, interaction strengths were only calculated for the first 300000 training samples. We created a composite importance metric for each predictor variable by dividing the Gini, PFI, LOCO, and SHAP metrics by the sum of their absolute values and then summing them.

For predictor variable x, at location ℓ on the latitude–longitude grid, the SHAP value with the largest magnitude out of all 12 months, m, was calculated as

$$\mathrm{SHAP}_{x,\ell} := \mathrm{SHAP}_{x,\ell,\mathrm{m}_{\max}}, \quad \text{where } \mathrm{m}_{\max} = \underset{\mathrm{m}\in\{1,2,\ldots,12\}}{\arg\max} |\mathrm{SHAP}_{x,\ell,\mathrm{m}}|. \tag{1}$$

Maximally significant timescales were then calculated by weighting the antecedent months, a, using SHAP magnitudes:

$$t_{\max,\mathrm{X},\ell} = \frac{\sum_{\mathrm{a},x} \mathrm{a}|\mathrm{SHAP}_{x,\ell}|}{\sum_{\mathrm{a},x} |\mathrm{SHAP}_{x,\ell}|} \quad \text{for a}, x \in \{(0,\mathrm{X}),(1,\mathrm{X\ 1M}),(3,\mathrm{X\ 3M}),(6,\mathrm{X\ 6M}),(9,\mathrm{X\ 9M})\}, \tag{2}$$

where X denotes the basis predictor variable for which to carry out the calculation (e.g. FAPAR).

Locations with too many significant antecedent months were ignored in order to visualise resulting relationships more reliably; for example, if both the current ($|\mathrm{SHAP}_{\mathrm{X},\ell}|$) and nine-month antecedent ($|\mathrm{SHAP}_{\mathrm{X\ 9M},\ell}|$) magnitudes are dominant, the weighted mean month (according to Eq. (2)) would lie in between which is physically meaningless. We designed an algorithm to detect SHAP values that differ significantly from the baseline in order to mitigate this. Additionally, we also employed a range-based threshold, whereby locations were ignored using the mean BA at location ℓ, $\overline{\mathrm{BA}}_\ell$ (based on all BA samples), if

$$\max_x(\mathrm{SHAP}_{x,\ell}) - \min_x(\mathrm{SHAP}_{x,\ell}) < 0.12 \times \overline{\mathrm{BA}}_\ell. \tag{3}$$

We further used Accumulated Local Effects (ALE) plots (Apley and Zhu, 2020) to examine and interpret the coupled relationships fitted by the RF models. ALE plots are a more robust alternative to partial dependence plots (PDP) or individual conditional expectation (ICE) plots (Apley and Zhu, 2020; Molnar, 2020). We assessed the impact of each of the predictor

https://doi.org/10.5194/bg-2020-409
Preprint. Discussion started: 11 November 2020

variables on BA in isolation using 1D ALEs, taking into account the effect of all other predictor variables. Underlying inhomogeneities may appear when the model fits different relationships for different locations. We tested for inhomogeneities by subsampling the dataset prior to ALE plot construction, allowing the visualisation of underlying relationships for a subset of locations and times. The causes of the inhomogeneities were explored using 2D ALE plots, which show the combined effect of two predictor variables on BA.

3 Results

The ALL model, which includes all 50 variables, achieves an R^2 of 0.884 for the training dataset and of 0.686 for the validation dataset (Fig. 1). Out-of-sample predictions on the validation set (Fig. 2b) show a similar geographic pattern to observed BA (Fig. 2a). However, overprediction in the validation set relative to observed BA is more widespread than underprediction (Fig. 2c). Nonetheless, there is no bias; the ALL model predicts a mean out-of-sample BA of 2.49×10^{-3} compared to the expected 2.48×10^{-3}. The apparent overprediction is the result of plotting relative (as opposed to absolute) errors, which amplifies the fact that the ALL model does not predict very low BA accurately: BA predictions are no lower than 2.22×10^{-5}, while the observed BA is 0 for 85.7% of samples. Generally, extreme BA is captured more poorly by the model than intermediate BA, leading to overprediction at low and underprediction at high BA values. More samples are over-predicted because there are more values with low BA than high BA, leading to many instances of slight overprediction balanced by few instances of comparatively large underprediction (Fig. S1, S2).

Climate variables and fuel-related vegetation indices have the strongest influence on BA in the ALL model (Table S2). Both current and antecedent conditions are important. Current DD and MaxT are ranked 1st and 3rd respectively, but antecedent DD also has a strong influence (DD 1M and DD 3M are ranked 6th and 7th in importance). Similarly, although current FAPAR is the most important vegetation index (2nd), with both current SIF and VOD occurring in the top 15 predictors, antecedent vegetation state also has a strong influence on BA. However, antecedent conditions $>$ 9M are unimportant in the ALL model. Vegetation characteristics such as the cover of specific plant types (TREE, SHRUB, HERB) or AGB are only moderately important in determining BA (all ranked below the top 15 predictors). Human impacts, as represented by CROP and POPD, are also only moderately important globally for BA, ranked respectively 13th and 15th. Natural ignitions, as represented by lightning are only ranked 26th, suggesting that at a global climatological scale burning is not limited by lightning.

The model using the top 15 predictors from the ALL model (TOP15) performs only marginally worse than the ALL model, with an R^2 of 0.876 for the training dataset and of 0.676 for the validation dataset. This nearly equivalent performance reflects the fact that there is a high degree of correlation between several of the variables (Fig. S3) included in the ALL model. The absolute values and difference between the R^2 for the training and validation datasets in the TOP15 and ALL models are effectively the same, implying that the inclusion of extra predictors in the ALL model does not improve predictive capability. The removal of predictor variables is however likely to reduce overfitting in the TOP15 model compared to the ALL model (Runge et al., 2019; Nowack et al., 2020)

https://doi.org/10.5194/bg-2020-409
Preprint. Discussion started: 11 November 2020

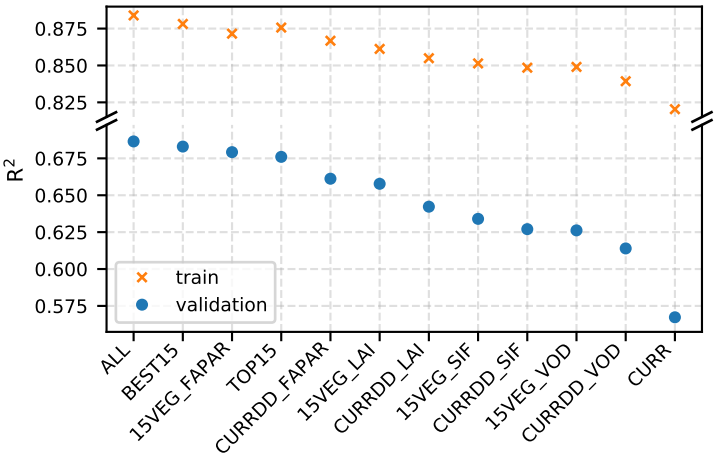

Figure 1. Global climatological R^2 scores for the different experiments.

The importance of antecedent fuel-related vegetation indices for predicting BA is corroborated by the results from the model that only includes predictors for the current month (CURR), where there is a large decrease in the R^2 for the validation dataset compared to either the ALL (-0.119) or TOP15 (-0.116) model. Comparison of the mean out-of-sample prediction error shows that 56% of grid cells are better predicted in the ALL model compared to the CURR model (Fig. 3). However, there does not appear to be any regional patterning in the improvement caused by including antecedent vegetation conditions. The decrease in the R^2 for the training dataset is smaller (–0.064) than for the validation dataset, indicating that overfitting may be more of a problem in the CURR model than the ALL model. Compared to the ALL model, fuel-related vegetation properties are less important in the CURR model: VOD is the highest-ranked vegetation variable but is only fifth in importance (Table S2).

The fuel-related vegetation variables included in the TOP15 model are correlated with one another (Fig. S3), and there are high correlations between these four variables on specific antecedent timescales. This suggests it may be unnecessary to include all these variables to capture the influence of fuel build-up on BA. Comparison of the models which only include current and antecedent conditions for one fuel-related vegetation variable (15VEG_FAPAR, 15VEG_LAI, 15VEG_VOD, 15VEG_SIF) confirms this. These models all perform better than the CURR model (Fig. 1). The 15VEG_FAPAR model performs better than the TOP15 model and almost as well as the ALL model. LAI appears to be a better predictor, considered on its own, than either SIF or VOD (Fig. 1). The 15VEG_FAPAR also has the lowest training–validation R^2 gap (0.192) of all the four models, which suggests that it has the most generalisable relationships. The importance of including antecedent DD is borne out by the comparison of these four experiments and the experiments which only included current DD (CURRDD_FAPAR, CURRDD_LAI, CURRDD_VOD, CURRDD_SIF). In each case, the predictions for the same vegetation predictor variable are worse (Fig. 1). The BEST 15 model contains the best combination of the fuel-related vegetation predictors (current FAPAR, FAPAR 1M, LAI 3M, SIF 6M, VOD 9M). The performance of this model, with a training R^2 of 0.878 and a validation R^2 of 0.683, is only bettered by the ALL model.

https://doi.org/10.5194/bg-2020-409
Preprint. Discussion started: 11 November 2020

Biogeosciences Discussions
Open Access
EGU

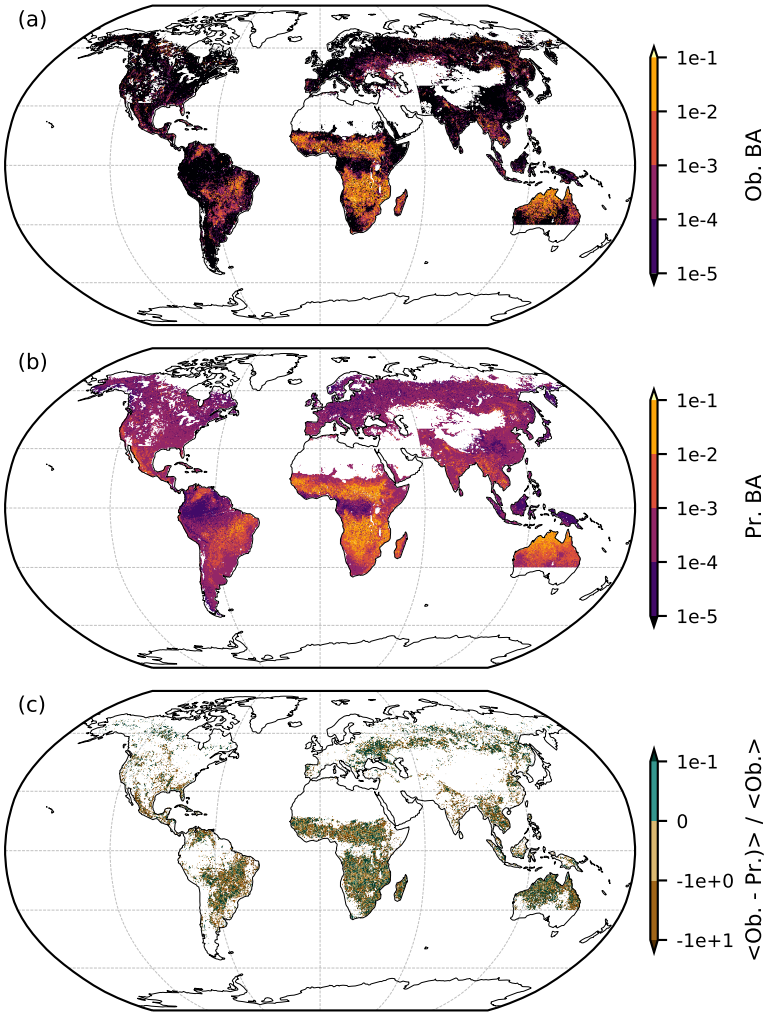

Figure 2. (a) Average observed (Ob.) BA derived from the GFED4 BA dataset (Giglio et al., 2013). (b) Out-of-sample predictions (Pr.) by the ALL model. (c) Relative prediction error of the ALL model calculated by taking the mean of the difference between observations and predictions divided by the mean observations. Areas with very low (or non-existent) observed BA (a) are omitted from (c) due to the effect of dividing by (nearly) zero.

Current and antecedent states of both fuel-related vegetation properties and DD have different impacts on BA (Fig. 4). Current FAPAR has a negative effect on BA (Fig. 4a), which is strongest at intermediate levels of FAPAR, while antecedent FAPAR has a positive effect on BA. The impact of antecedent FAPAR is strongest for the preceding 1 month but persists for up to 6 months; longer lags tend to produce results more similar to the current relationship because of autocorrelation at the yearly
255 scale. Current DD has a positive effect on BA (Fig. 4b), while antecedent DD has a generally negative effect except if DD is very high when the effect becomes positive again. Whereas the positive antecedent effect of FAPAR on BA is strongest for the

https://doi.org/10.5194/bg-2020-409
Preprint. Discussion started: 11 November 2020

Biogeosciences Discussions Open Access EGU

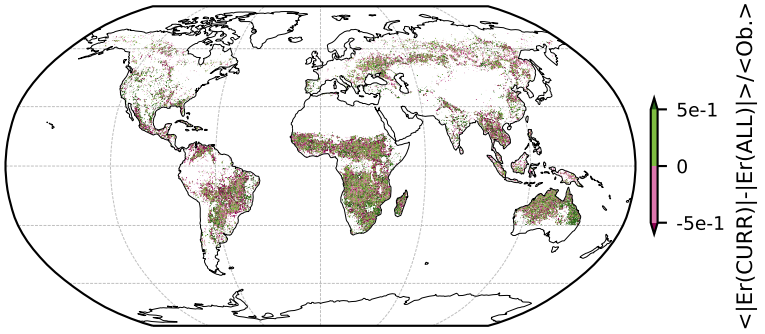

Figure 3. Mean change in out-of-sample prediction error between the CURR and ALL models, relative to mean observations (<Ob.>). Green regions have decreased prediction error using the ALL model compared to the CURR model, and vice versa for the purple regions. Areas with high BA (see Fig. 2a) tend to experience lower changes in relative prediction error.

preceding 1M relationship, the negative impact becomes gradually stronger with antecedent DD up to 9M. These relationships make intuitive sense: whereas high antecedent levels of FAPAR suggest that fuel availability is not a limiting factor, high FAPAR in the current month indicates that the vegetation has sufficient moisture to be actively growing and therefore is less likely to burn. In contrast, dry conditions in the current month promote fire whereas dry conditions in preceding months reduce vegetation growth and hence fuel build-up. Although prolonged droughts might be expected to reduce the availability of fuel, the positive relationship between BA and DD at very high levels of DD across all antecedent states does not support this expectation. The positive impact of drought in the current month becomes apparent for dry days $> \sim 10$ days, whereas the threshold is higher for antecedent months: BA only increases when the number of dry days is $> \sim 20$ days for the preceding month (DD 1M) and requires $> \sim 40$ days for DD 9M. This suggests that positive large antecedent DD may reflect prolonged droughts extending into the current month, thereby increasing fuel flammability and promoting fire.

The relationships between current or antecedent conditions and BA are generally reproduced in all of the RF models (Fig. 4, 5, S4). However, exclusion of antecedent vegetation predictors can lead to counter-intuitive relationships between the current vegetation state and BA. Although the CURR model produces the expected relationship between current FAPAR (and SIF; Fig. 5a, S4a), the relationship between current LAI (and VOD) and BA is initially positive and then flat (Fig. 5b, S4b). This model does not show the strong negative relationship between current LAI and BA that occurs when antecedent moisture and vegetation conditions are included.

Although it is informative to consider the impact of individual predictor variables on BA, the expression of these relationships in the real world is likely to be conditioned by interactions with other variables. For example, low values of current FAPAR are associated with high BA (Fig. 4a), but this association occurs only when antecedent FAPAR is high (Fig. 6). Low FAPAR in the current month reflects unsuitable conditions for plant growth, for example during the dry season, and fuel build-up during the preceding months is therefore a prerequisite for fire to occur. The strong autocorrelation between current and preceding FAPAR values means that the occurrence of low current FAPAR coupled with high antecedent FAPAR is not widespread, being largely

https://doi.org/10.5194/bg-2020-409
Preprint. Discussion started: 11 November 2020

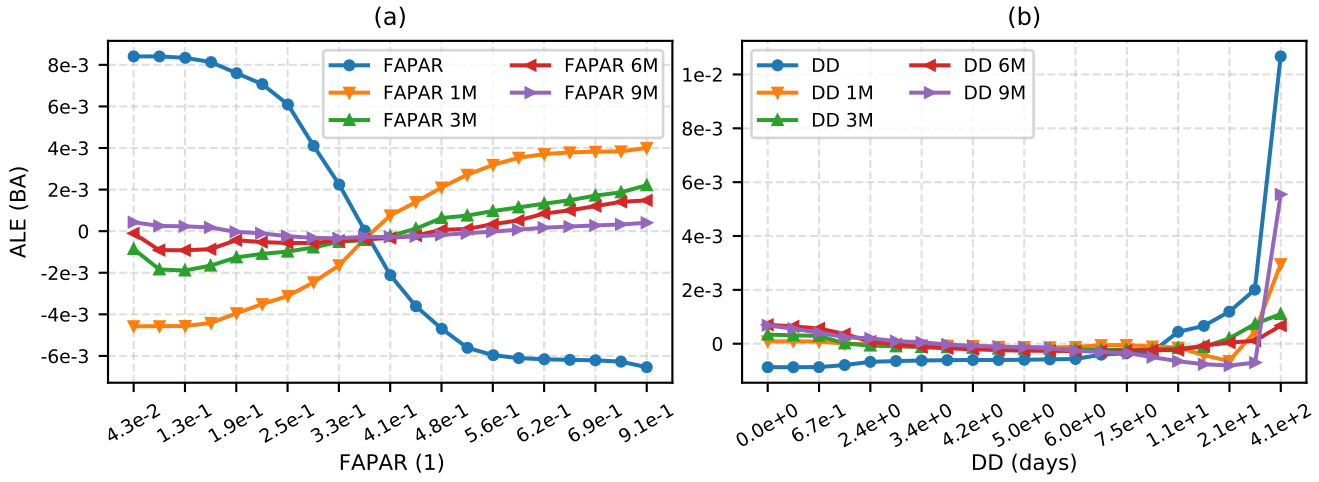

Figure 4. First-order ALEs for different antecedent (< 1 yr) relationships with (a) FAPAR and (b) DD in the 15VEG_FAPAR model, showing the underlying relationships with BA after accounting for all other variables. Evenly spaced quantiles were used in the construction of the plots. Labels were calculated using the averaged quantiles of all the datasets used.

confined to shrublands in Africa. However, there is a significant interaction between current DD and current FAPAR (Fig. S5), with positive reinforcement of their influence on BA when DD is high and FAPAR is low and a negative influence on BA when DD is high and FAPAR is high. Increased BA for high DD and low FAPAR is consistent with strong drought-induced fire in low productivity environments of sub-Saharan Africa, northern Australia, and isolated regions bordering the African tropical rainforests. Decreased BA as a result of increased DD and increased FAPAR is likely a sign of high-productivity environments that are not fire-prone, despite occasional drought.

The timescales of both fuel build-up and fuel drying are influenced by fuel type and are therefore expected to vary across biomes. Current fuel-related vegetation properties, such as FAPAR (Fig. 7a), have an important effect in tropical regions, particularly dry tropical regions, but are less important in temperate forest regions. Antecedent FAPAR (Fig. 7b) is important in most regions, with the strongest influence from the antecedent 3–6 months. Current DD (Fig. 7c) is generally more important than antecedent DD, although the impact on BA varies geographically: tropical and boreal regions show decreased BA as a result of low current DD, while northwestern Australia, extra-tropical Africa, the Cerrado of Brazil, and the western USA experience increased burning as a result of low DD (Fig. S6). The timescale on which antecedent drought affects BA (Fig. 7d) is more variable than that for fuel-related vegetation properties, ranging from 1–3 months in boreal forests, parts of sub-Saharan Africa, and northern Australia, to $\sim$4 months in the tropics, and $\sim$6 months or longer in more arid regions.

https://doi.org/10.5194/bg-2020-409
Preprint. Discussion started: 11 November 2020

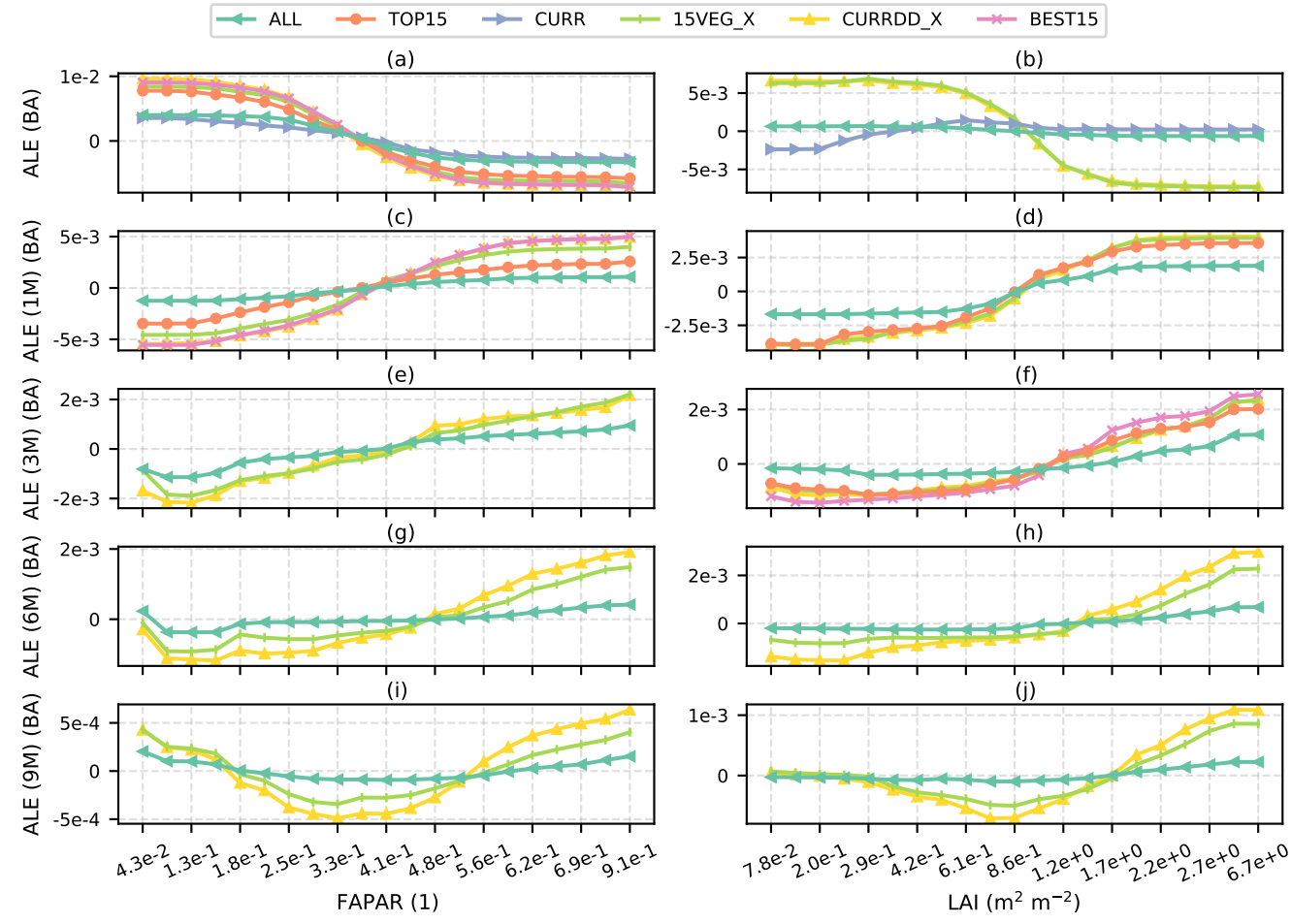

Figure 5. First-order LAI ALEs for different lags (< 1 yr) from all relevant modelling experiments for the relationships between BA and FAPAR (left hand column) and LAI (right hand column). Evenly spaced quantiles were used in the construction of the plots. Labels were calculated using the averaged quantiles of all the datasets used.

4 Discussion

Many studies have shown that climate, vegetation properties, and human factors are all important predictors of BA (e.g. Aldersley et al., 2011; Bistinas et al., 2014; Forkel et al., 2017, 2019a). Although spatial variation in BA is predominantly the result of spatial variability in moisture and fuel-load (Archibald et al., 2009), there is still poor understanding of the critical timescales for fuel build-up and fuel drying. We have shown that the inclusion of both antecedent vegetation conditions that influence fuel build-up and antecedent conditions that influence fuel drying are necessary for the accurate prediction of BA. While conditions in the year before a fire are important, antecedent conditions for intervals > 1 yr do not have a significant impact on BA in our analyses. A similar conclusion was reached by Forkel et al. (2017). The critical timescale for fuel build-up

https://doi.org/10.5194/bg-2020-409
Preprint. Discussion started: 11 November 2020

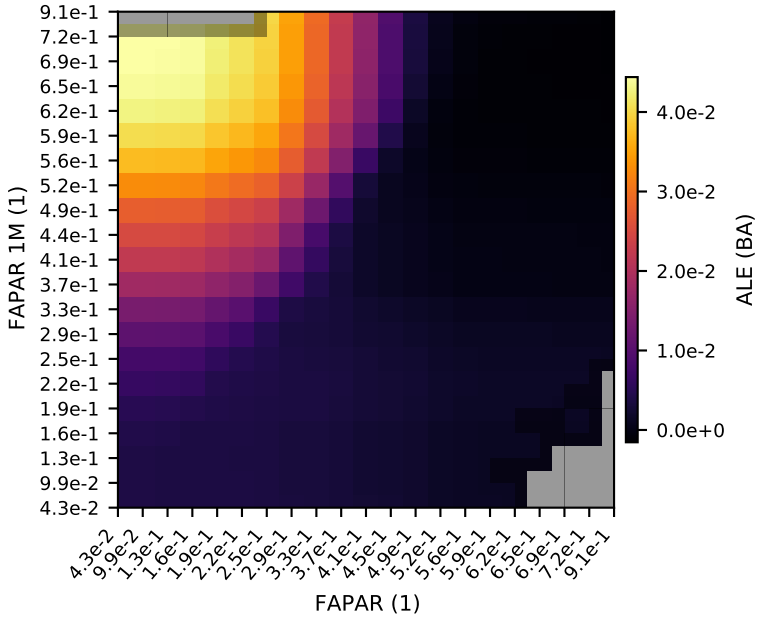

Figure 6. Second-order ALE plot showing the combined zeroth order (mean), first order, and second order modelled effects of FAPAR and FAPAR 1M on BA from the 15VEG_FAPAR model, taking into account all other variables. Grey boxes indicate missing data. See Fig. S7 for the sample count matrix which demonstrates the correlation between the variables and thus shows that samples are unlikely to fall into the top-left bins. Evenly spaced quantiles are used in the construction and labelling of the plots.

varies with vegetation type, with longer timescales being more important in temperate regions and recent conditions being more important in the tropics. The effect of vegetation variables is also biome-dependent because of differing climatic constraints. The length of the dry-day period in the current month has the largest impact on BA but antecedent DD can also be important, particularly in temperate regions.

The finding that fuel build-up on timescales longer than a year is not an important predictor of BA is surprising, given that fuel build-up as a result of fire suppression has been linked to large and catastrophic fires (e.g. in the United States; Marlon et al., 2012; Parks et al., 2015; Higuera et al., 2015). The failure to detect an influence of longer-term fuel build-up on BA probably reflects the short time interval ($\sim$5 yrs) used for the analyses because of the requirement that all of the datasets were available for the same time period. The seasonal differences captured by our analyses may be unimportant in regions where long fire return times (or fire suppression) allow fuel build-up over longer periods. Wetter forests with long fire-return intervals may also be more affected by longer term moisture deficits (Abatzoglou and Kolden, 2013) that are not captured in the limited time period analysed. It would be worthwhile re-examining the influence of longer timescales on BA in the future, when longer datasets are available.

We have shown that it is not necessary to include multiple fuel-related vegetation variables in order to predict BA, provided that both current and antecedent conditions are taken into consideration. According to our analyses, FAPAR is the best

https://doi.org/10.5194/bg-2020-409
Preprint. Discussion started: 11 November 2020

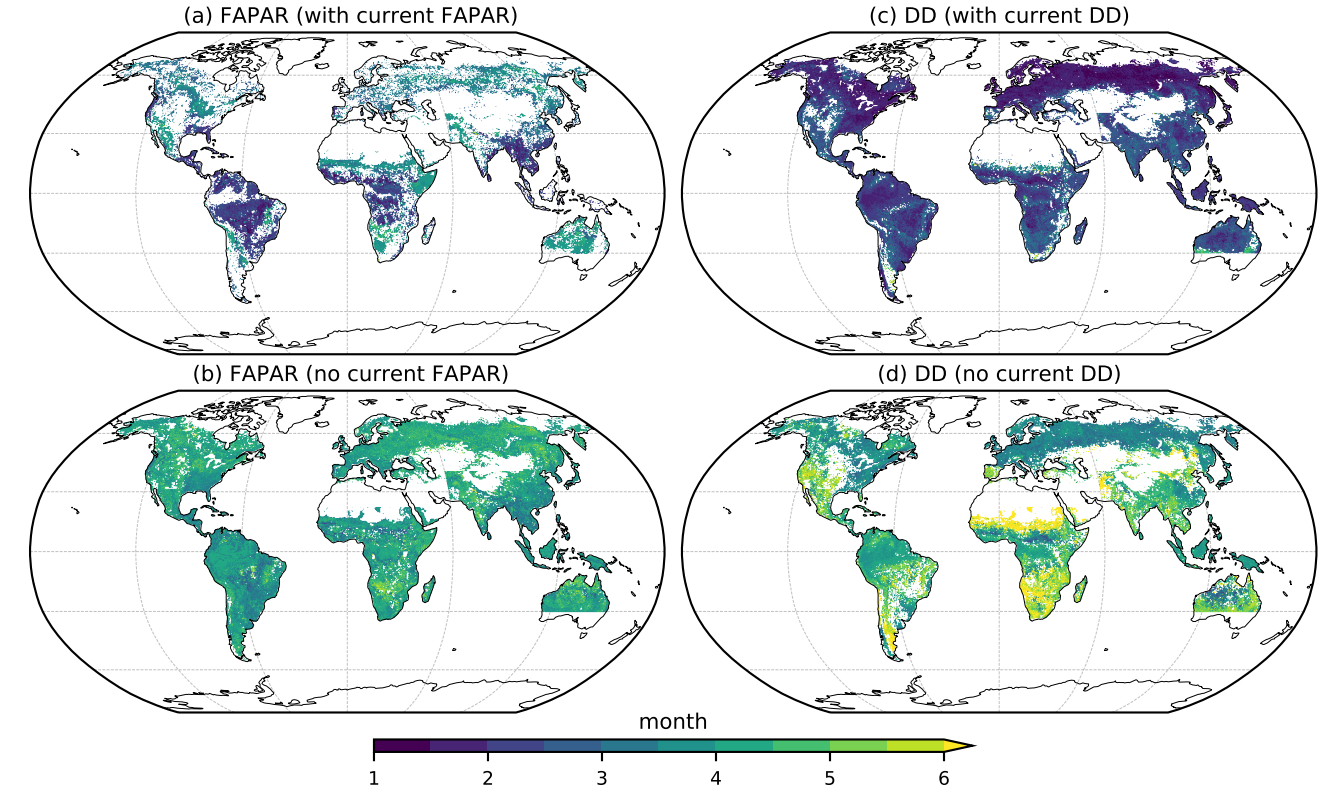

Figure 7. Timescales of influence of FAPAR and DD on BA. The plots show the period that is most important for determining BA from the 15VEG_FAPAR model for (a) FAPAR and (c) DD. Plots (b) and (d) show which of the antecedent periods is most important (i.e. disregarding the influence of current conditions) in these experiments. Note that the maps give no indication about the sign of the influence of the predictor on BA (see Fig. S6).

fuel-related vegetation predictor. However, all four fuel-related vegetation predictors produce reasonable results, and other predictors (e.g. VOD) have been found to be important in other studies (e.g. Forkel et al., 2017). Optimising the timescales of different fuel-related vegetation predictors suggests that FAPAR is most important on short timescales (current, 1M) and the other vegetation properties appear to be more useful on longer timeframes. The good performance of models including FAPAR is due to the fact that the parts of the world responding most strongly to FAPAR and FAPAR 1M tend to be fuel-limited, dry biomes accounting for the majority of global BA (Giglio et al., 2013). Therefore, globally averaged model performance metrics will tend to favour model predictor variables which best represent these dominant fire regimes.

Our analyses are impacted by the influence of previous fires on current vegetation conditions. Burnt grid cells could have a lower FAPAR, for example, as a result of prior burning in the current month. This is a problem, related to the temporal and spatial scales of the analysis, because we are solely interested in how pre-fire vegetation conditions affect BA. A monthly analysis cannot resolve processes that occur on the order of only a few days, while the impact of previous fires on spatially

https://doi.org/10.5194/bg-2020-409
Preprint. Discussion started: 11 November 2020

averaged vegetation properties is proportional to the fraction of the grid cell that is burnt. In savannah regions of Africa and northern Australia, where on average up to 10% of a 0.25° grid cell burns in any given month, this could have a significant effect on the averaged values of vegetation properties used in our analyses. Using a finer spatial scale for analysis would counteract the impact of spatial smoothing, allowing burnt pixels to be ignored and predictor values to be estimated only from unburnt cells. Using a finer temporal resolution would allow the calculation of predictor variables only up to the time of burning. In practice, however, the lack of accurate fire statistics at finer scales (Abatzoglou and Kolden, 2013) limits the temporal and spatial resolution that could usefully be achieved.

Although the limitation of the spatial (and temporal) resolution of the observations could impact the realism of the RF model, as could the omission of variables that affect fuel build-up, the consistency of the vegetation relationships shown by all the models including antecedent conditions indicates that processes related to fuel build-up are adequately represented by the chosen set of predictors.

5 Conclusions

The dependence of BA on multiple climatic and biophysical variables has been modelled using a random forest algorithm. We showed that FAPAR was the most significant vegetation variable, and dry-day period and maximum temperature the most significant climatic variables, influencing BA. The inclusion of antecedent relationships with FAPAR and dry-day period significantly improved model performance. Antecedent relationships to BA were consistently different from instantaneous relationships, with the spatiotemporal variation of fuel build-up processes apparent via the relative importance of these different lagged relationships. A clear contrast between fuel- and moisture-limited regions was identified using the spatial variation of the relationship between antecedent FAPAR and BA. Moisture-limited regions were more strongly affected by suppression of fire at instantaneous timescales, while fuel-limited regions were most affected by fuel build-up over the previous $\sim$4 months. The instantaneous dry-day period was found to have the biggest effect on BA, suppressing or promoting fire based on the climate.

Code availability. Computer code can be found in the fuel-build-up package (Kuhn-Regnier, 2020b). ALE plots were generated using the ALEPython package (Kuhn-Regnier et al., 2020). Data analysis was carried out using the Python 3.7 (Van Rossum and Drake, 2009) packages SciPy (Virtanen et al., 2020), Matplotlib (Hunter, 2007), NumPy (Oliphant, 2006), Iris (Met Office, 2010), Dask (Dask Development Team, 2016), Jupyter notebooks (Kluyver et al., 2016), wildfires (Kuhn-Regnier, 2020c), and era5analysis (Kuhn-Regnier, 2020a). GFED4 data was read using pyhdf (https://github.com/fhs/pyhdf, wraps NCSA HDF version 4).

Author contributions. Conceptualization, AKR, AV, ICP, SPH; Methodology, AKR; Software, AKR; Validation, AKR; Formal Analysis, AKR; Investigation, AKR, SPH; Data Curation, AKR, MF; Writing – Original Draft, AKR; Writing – Review & Editing, AKR, AV, PN, MF, ICP, SPH; Visualization, AKR; Supervision, AV, PN, ICP, SPH.

https://doi.org/10.5194/bg-2020-409
Preprint. Discussion started: 11 November 2020

Competing interests. The authors declare that they have no conflict of interest.

Acknowledgements. AKR acknowledges support from the NERC Centre for Doctoral Training in Quantitative and Modelling skills in Ecology and Evolution (QMEE, grant reference NE/P012345/1). ICP acknowledges support from the ERC-funded project REALM (grant number 787203). SPH acknowledges support from the ERC-funded project GC2.0 (Global Change 2.0: Unlocking the past for a clearer future, grant number 694481). This research was partially funded by the Leverhulme Centre for Wildfires, Environment, and Society through the Leverhulme Trust, grant number RC-2018-023.

https://doi.org/10.5194/bg-2020-409
Preprint. Discussion started: 11 November 2020

References

Abatzoglou, J. T. and Kolden, C. A.: Relationships between Climate and Macroscale Area Burned in the Western United States, Int. J. Wildland Fire, 22, 1003–1020, https://doi.org/10.1071/WF13019, 2013.

Abatzoglou, J. T. and Williams, A. P.: Impact of Anthropogenic Climate Change on Wildfire across Western US Forests, Proc Natl Acad Sci USA, 113, 11 770–11 775, https://doi.org/10.1073/pnas.1607171113, 2016.

Abatzoglou, J. T., Williams, A. P., Boschetti, L., Zubkova, M., and Kolden, C. A.: Global Patterns of Interannual Climate-Fire Relationships, Glob Change Biol, 24, 5164–5175, https://doi.org/10.1111/gcb.14405, 2018.

Abatzoglou, J. T., Williams, A. P., and Barbero, R.: Global Emergence of Anthropogenic Climate Change in Fire Weather Indices, Geophys. Res. Lett., 46, 326–336, https://doi.org/10.1029/2018GL080959, 2019.

Albergel, C., Rüdiger, C., Pellarin, T., Calvet, J.-C., Fritz, N., Froissard, F., Suquia, D., Petitpa, A., Piguet, B., and Martin, E.: From Near-Surface to Root-Zone Soil Moisture Using an Exponential Filter: An Assessment of the Method Based on in-Situ Observations and Model Simulations, Hydrol. Earth Syst. Sci., 12, 1323–1337, https://doi.org/10.5194/hess-12-1323-2008, 2008.

Aldersley, A., Murray, S. J., and Cornell, S. E.: Global and Regional Analysis of Climate and Human Drivers of Wildfire, Science of The Total Environment, 409, 3472–3481, https://doi.org/10.1016/j.scitotenv.2011.05.032, 2011.

Alvarado, S. T., Andela, N., Silva, T. S. F., and Archibald, S.: Thresholds of Fire Response to Moisture and Fuel Load Differ between Tropical Savannas and Grasslands across Continents, Global Ecol Biogeogr, 29, 331–344, https://doi.org/10.1111/geb.13034, 2020.

Andela, N., Morton, D. C., Giglio, L., Chen, Y., van der Werf, G. R., Kasibhatla, P. S., DeFries, R. S., Collatz, G. J., Hantson, S., Kloster, S., Bachelet, D., Forrest, M., Lasslop, G., Li, F., Mangeon, S., Melton, J. R., Yue, C., and Randerson, J. T.: A Human-Driven Decline in Global Burned Area, Science, 356, 1356–1362, https://doi.org/10.1126/science.aal4108, 2017.

Apley, D. W. and Zhu, J.: Visualizing the Effects of Predictor Variables in Black Box Supervised Learning Models, J. R. Stat. Soc. Ser. B Stat. Methodol., 82, 1059–1086, https://doi.org/10.1111/rssb.12377, 2020.

Archibald, S., Roy, D. P., van Wilgen, B. W., and Scholes, R. J.: What Limits Fire? An Examination of Drivers of Burnt Area in Southern Africa, Glob. Change Biol., 15, 613–630, https://doi.org/10.1111/j.1365-2486.2008.01754.x, 2009.

Avitabile, V., Herold, M., Heuvelink, G. B. M., Lewis, S. L., Phillips, O. L., Asner, G. P., Armston, J., Ashton, P. S., Banin, L., Bayol, N., Berry, N. J., Boeckx, P., de Jong, B. H. J., DeVries, B., Girardin, C. A. J., Kearsley, E., Lindsell, J. A., Lopez-Gonzalez, G., Lucas, R., Malhi, Y., Morel, A., Mitchard, E. T. A., Nagy, L., Qie, L., Quinones, M. J., Ryan, C. M., Ferry, S. J. W., Sunderland, T., Laurin, G. V., Gatti, R. C., Valentini, R., Verbeeck, H., Wijaya, A., and Willcock, S.: An Integrated Pan-Tropical Biomass Map Using Multiple Reference Datasets, Glob. Change Biol., 22, 1406–1420, https://doi.org/10.1111/gcb.13139, 2016.

Barbero, R., Abatzoglou, J. T., Larkin, N. K., Kolden, C. A., and Stocks, B.: Climate Change Presents Increased Potential for Very Large Fires in the Contiguous United States, Int. J. Wildland Fire, 24, 892–899, https://doi.org/10.1071/WF15083, 2015.

Bedia, J., Herrera, S., Gutiérrez, J. M., Benali, A., Brands, S., Mota, B., and Moreno, J. M.: Global Patterns in the Sensitivity of Burned Area to Fire-Weather: Implications for Climate Change, Agricultural and Forest Meteorology, 214-215, 369–379, https://doi.org/10.1016/j.agrformet.2015.09.002, 2015.

Bistinas, I., Harrison, S. P., Prentice, I. C., and Pereira, J. M. C.: Causal Relationships versus Emergent Patterns in the Global Controls of Fire Frequency, Biogeosciences, 11, 5087–5101, https://doi.org/10.5194/bg-11-5087-2014, 2014.

https://doi.org/10.5194/bg-2020-409
Preprint. Discussion started: 11 November 2020

Bowman, D. M. J. S., Balch, J., Artaxo, P., Bond, W. J., Cochrane, M. A., D'Antonio, C. M., DeFries, R., Johnston, F. H., Keeley, J. E., Krawchuk, M. A., Kull, C. A., Mack, M., Moritz, M. A., Pyne, S., Roos, C. I., Scott, A. C., Sodhi, N. S., and Swetnam, T. W.: The Human Dimension of Fire Regimes on Earth, J. Biogeogr., 38, 2223–2236, https://doi.org/10.1111/j.1365-2699.2011.02595.x, 2011.

Bowman, D. M. J. S., Williamson, G. J., Abatzoglou, J. T., Kolden, C. A., Cochrane, M. A., and Smith, A. M. S.: Human Exposure and Sensitivity to Globally Extreme Wildfire Events, Nat. Ecol. Evol., 1, 1–6, https://doi.org/10.1038/s41559-016-0058, 2017.

Breiman, L.: Random Forests, Machine Learning, 45, 5–32, https://doi.org/10.1023/A:1010933404324, 2001.

Burton, C., Betts, R. A., Jones, C. D., and Williams, K.: Will Fire Danger Be Reduced by Using Solar Radiation Management to Limit Global Warming to 1.5 °C Compared to 2.0 °C?, Geophys. Res. Lett., 45, 3644–3652, https://doi.org/10.1002/2018GL077848, 2018.

Copernicus Climate Change Service (C3S): ERA5: Fifth Generation of ECMWF Atmospheric Reanalyses of the Global Climate . Copernicus Climate Change Service Climate Data Store (CDS), https://cds.climate.copernicus.eu/cdsapp#!/home, 2017.

Dask Development Team: Dask: Library for Dynamic Task Scheduling, 2016.

Dormann, C. F., Elith, J., Bacher, S., Buchmann, C., Carl, G., Carré, G., Marquéz, J. R. G., Gruber, B., Lafourcade, B., Leitão, P. J., Münkemüller, T., McClean, C., Osborne, P. E., Reineking, B., Schröder, B., Skidmore, A. K., Zurell, D., and Lautenbach, S.: Collinearity: A Review of Methods to Deal with It and a Simulation Study Evaluating Their Performance, Ecography, 36, 27–46, https://doi.org/10.1111/j.1600-0587.2012.07348.x, 2013.

Forkel, M., Dorigo, W., Lasslop, G., Teubner, I., Chuvieco, E., and Thonicke, K.: A Data-Driven Approach to Identify Controls on Global Fire Activity from Satellite and Climate Observations (SOFIA V1), Geosci. Model Dev., 10, 4443–4476, https://doi.org/10.5194/gmd-10-4443-2017, 2017.

Forkel, M., Andela, N., Harrison, S. P., Lasslop, G., van Marle, M., Chuvieco, E., Dorigo, W., Forrest, M., Hantson, S., Heil, A., Li, F., Melton, J., Sitch, S., Yue, C., and Arneth, A.: Emergent Relationships on Burned Area in Global Satellite Observations and Fire-Enabled Vegetation Models, Biogeosciences Discuss., pp. 1–31, https://doi.org/10.5194/bg-2018-427, 2019a.

Forkel, M., Dorigo, W., Lasslop, G., Chuvieco, E., Hantson, S., Heil, A., Teubner, I., Thonicke, K., and Harrison, S. P.: Recent Global and Regional Trends in Burned Area and Their Compensating Environmental Controls, Environ. Res. Commun., 1, 051 005, https://doi.org/10.1088/2515-7620/ab25d2, 2019b.

Giglio, L., Randerson, J. T., and van der Werf, G. R.: Analysis of Daily, Monthly, and Annual Burned Area Using the Fourth-Generation Global Fire Emissions Database (GFED4), J. Geophys. Res. Biogeosciences, 118, 317–328, https://doi.org/10.1002/jgrg.20042, 2013.

Goss, M., Swain, D. L., Abatzoglou, J. T., Sarhadi, A., Kolden, C., Williams, A. P., and Diffenbaugh, N. S.: Climate Change Is Increasing the Risk of Extreme Autumn Wildfire Conditions across California, Environ. Res. Lett., https://doi.org/10.1088/1748-9326/ab83a7, 2020.

Hantson, S., Kelley, D. I., Arneth, A., Harrison, S. P., Archibald, S., Bachelet, D., Forrest, M., Hickler, T., Lasslop, G., Li, F., Mangeon, S., Melton, J. R., Nieradzik, L., Rabin, S. S., Prentice, I. C., Sheehan, T., Sitch, S., Teckentrup, L., Voulgarakis, A., and Yue, C.: Quantitative Assessment of Fire and Vegetation Properties in Historical Simulations with Fire-Enabled Vegetation Models from the Fire Model Intercomparison Project, Preprint, Biogeosciences, https://doi.org/10.5194/gmd-2019-261, 2020.

Harris, I., Jones, P., Osborn, T., and Lister, D.: Updated High-resolution Grids of Monthly Climatic Observations – the CRU TS3.10 Dataset, Int. J. Climatol., 34, 623–642, https://doi.org/10.1002/joc.3711, 2014.

Higuera, P. E., Abatzoglou, J. T., Littell, J. S., and Morgan, P.: The Changing Strength and Nature of Fire-Climate Relationships in the Northern Rocky Mountains, U.S.A., 1902-2008, PLOS ONE, 10, e0127 563, https://doi.org/10.1371/journal.pone.0127563, 2015.

Hooker, G. and Mentch, L.: Please Stop Permuting Features: An Explanation and Alternatives, ArXiv190503151 Cs Stat, 2019.

Hunter, J. D.: Matplotlib: A 2D Graphics Environment, Comput. Sci. Eng., 9, 90–95, 2007.

https://doi.org/10.5194/bg-2020-409
Preprint. Discussion started: 11 November 2020

Jolly, W. M., Cochrane, M. A., Freeborn, P. H., Holden, Z. A., Brown, T. J., Williamson, G. J., and Bowman, D. M. J. S.: Climate-Induced Variations in Global Wildfire Danger from 1979 to 2013, Nat. Commun., 6, 7537, https://doi.org/10.1038/ncomms8537, 2015.

Kaplan, J. O. and Lau, H.-K.: The WGLC Global Gridded Monthly Lightning Stroke Density and Climatology, https://doi.org/10.1594/PANGAEA.904253, 2019.

Keane, R. E., Burgan, R., and van Wagtendonk, J.: Mapping Wildland Fuels for Fire Management across Multiple Scales: Integrating Remote Sensing, GIS, and Biophysical Modeling, Int. J. Wildland Fire, 10, 301, https://doi.org/10.1071/WF01028, 2001.

Kelley, D. I., Bistinas, I., Whitley, R., Burton, C., Marthews, T. R., and Dong, N.: How Contemporary Bioclimatic and Human Controls Change Global Fire Regimes, Nat. Clim. Chang., 9, 690–696, https://doi.org/10.1038/s41558-019-0540-7, 2019.

Klein Goldewijk, C.: Anthropogenic Land-Use Estimates for the Holocene; HYDE 3.2, https://doi.org/10.17026/DANS-25G-GEZ3, 2017.

Kloster, S. and Lasslop, G.: Historical and Future Fire Occurrence (1850 to 2100) Simulated in CMIP5 Earth System Models, Global and Planetary Change, 150, 58–69, https://doi.org/10.1016/j.gloplacha.2016.12.017, 2017.

Kloster, S., Mahowald, N. M., Randerson, J. T., and Lawrence, P. J.: The Impacts of Climate, Land Use, and Demography on Fires during the 21st Century Simulated by CLM-CN, Biogeosciences, 9, 509–525, https://doi.org/10.5194/bg-9-509-2012, 2012.

Kluyver, T., Ragan-Kelley, B., Pérez, F., Granger, B., Bussonnier, M., Frederic, J., Kelley, K., Hamrick, J., Grout, J., Corlay, S., Ivanov, P., Avila, D., Abdalla, S., and Willing, C.: Jupyter Notebooks – a Publishing Format for Reproducible Computational Workflows, in: Positioning and Power in Academic Publishing: Players, Agents and Agendas, edited by Loizides, F. and Schmidt, B., pp. 87–90, IOS Press, 2016.

Knorr, W., Jiang, L., and Arneth, A.: Climate, CO_2 and Human Population Impacts on Global Wildfire Emissions, Biogeosciences, 13, 267–282, https://doi.org/10.5194/bg-13-267-2016, 2016.

Köhler, P., Guanter, L., and Joiner, J.: A Linear Method for the Retrieval of Sun-Induced Chlorophyll Fluorescence from GOME-2 and SCIAMACHY Data, Atmospheric Meas. Tech., 8, 2589–2608, https://doi.org/10.5194/amt-8-2589-2015, 2015.

Kuhn-Regnier, A.: era5analysis, Zenodo, https://doi.org/10.5281/zenodo.4173493, 2020a.

Kuhn-Regnier, A.: fuel-build-up, Zenodo, https://doi.org/10.5281/zenodo.4167733, 2020b.

Kuhn-Regnier, A.: wildfires, Zenodo, https://doi.org/10.5281/zenodo.4167172, 2020c.

Kuhn-Regnier, A., Jumelle, M., and Rajaratnam, S.: ALEPython, Zenodo, https://doi.org/10.5281/zenodo.4171102, 2020.

Lasslop, G., Coppola, A. I., Voulgarakis, A., Yue, C., and Veraverbeke, S.: Influence of Fire on the Carbon Cycle and Climate, Curr Clim Change Rep, 5, 112–123, https://doi.org/10.1007/s40641-019-00128-9, 2019.

Li, W., MacBean, N., Ciais, P., Defourny, P., Lamarche, C., Bontemps, S., Moreau, I., Houghton, R. A., and Peng, S.: Gross and Net Land Cover Changes in the Main Plant Functional Types Derived from the Annual ESA CCI Land Cover Maps (1992–2015), Earth Syst. Sci. Data, 10, 219–234, https://doi.org/10.5194/essd-10-219-2018, 2018.

Lundberg, S. and Lee, S.-I.: A Unified Approach to Interpreting Model Predictions, in: Advances in Neural Information Processing Systems, edited by Guyon, I., Fergus, R., Wallach, H., von Luxburg, U., Garnett, R., Vishwanathan, S., and Bengio, S., vol. 2017-December, pp. 4766–4775, Neural information processing systems foundation, 2017.

Lundberg, S. M., Erion, G., Chen, H., DeGrave, A., Prutkin, J. M., Nair, B., Katz, R., Himmelfarb, J., Bansal, N., and Lee, S.-I.: From Local Explanations to Global Understanding with Explainable AI for Trees, Nat. Mach. Intell., 2, 56–67, https://doi.org/10.1038/s42256-019-0138-9, 2020.

Mansfield, L. A., Nowack, P. J., Kasoar, M., Everitt, R. G., Collins, W. J., and Voulgarakis, A.: Predicting Global Patterns of Long-Term Climate Change from Short-Term Simulations Using Machine Learning, Npj Clim. Atmospheric Sci., 2020.

https://doi.org/10.5194/bg-2020-409
Preprint. Discussion started: 11 November 2020

Marlon, J. R., Bartlein, P. J., Gavin, D. G., Long, C. J., Anderson, R. S., Briles, C. E., Brown, K. J., Colombaroli, D., Hallett, D. J., Power, M. J., Scharf, E. A., and Walsh, M. K.: Long-Term Perspective on Wildfires in the Western USA, PNAS, 109, E535–E543, https://doi.org/10.1073/pnas.1112839109, 2012.

Martínez, J., Vega-Garcia, C., and Chuvieco, E.: Human-Caused Wildfire Risk Rating for Prevention Planning in Spain, Journal of Environmental Management, 90, 1241–1252, https://doi.org/10.1016/j.jenvman.2008.07.005, 2009.

Met Office: Iris: A Python Library for Analysing and Visualising Meteorological and Oceanographic Data Sets, Exeter, Devon, v2.4 edn., 2010.

Moesinger, L., Dorigo, W., De Jeu, R., Van der Schalie, R., Scanlon, T., Teubner, I., and Forkel, M.: The Global Long-Term Microwave Vegetation Optical Depth Climate Archive VODCA (Version 1.0) [Data Set], https://doi.org/10.5281/zenodo.2575599, 2019.

Moesinger, L., Dorigo, W., de Jeu, R., van der Schalie, R., Scanlon, T., Teubner, I., and Forkel, M.: The Global Long-Term Microwave Vegetation Optical Depth Climate Archive (VODCA), Earth Syst. Sci. Data, 12, 177–196, https://doi.org/10.5194/essd-12-177-2020, 2020.

Mohammed, G. H., Colombo, R., Middleton, E. M., Rascher, U., van der Tol, C., Nedbal, L., Goulas, Y., Pérez-Priego, O., Damm, A., Meroni, M., Joiner, J., Cogliati, S., Verhoef, W., Malenovský, Z., Gastellu-Etchegorry, J.-P., Miller, J. R., Guanter, L., Moreno, J., Moya, I., Berry, J. A., Frankenberg, C., and Zarco-Tejada, P. J.: Remote Sensing of Solar-Induced Chlorophyll Fluorescence (SIF) in Vegetation: 50 years of Progress, Remote Sensing of Environment, 231, 111 177, https://doi.org/10.1016/j.rse.2019.04.030, 2019.

Molnar, C.: Interpretable Machine Learning, 2020.

Myneni, R., Knyazikhin, Y., and Park, T.: MOD15A2H MODIS/Terra Leaf Area Index/FPAR 8-Day L4 Global 500m SIN Grid V006, https://doi.org/10.5067/MODIS/MOD15A2H.006, 2015.

Nowack, P., Braesicke, P., Haigh, J., Abraham, N. L., Pyle, J., and Voulgarakis, A.: Using Machine Learning to Build Temperature-Based Ozone Parameterizations for Climate Sensitivity Simulations, Environ. Res. Lett., 13, 104 016, https://doi.org/10.1088/1748-9326/aae2be, 2018.

Nowack, P., Runge, J., Eyring, V., and Haigh, J. D.: Causal Networks for Climate Model Evaluation and Constrained Projections, Nat. Commun., 11, 1415, https://doi.org/10.1038/s41467-020-15195-y, 2020.

Ogutu, B. O., Dash, J., and Dawson, T. P.: Evaluation of the Influence of Two Operational Fraction of Absorbed Photosynthetically Active Radiation (FAPAR) Products on Terrestrial Ecosystem Productivity Modelling, Int. J. Remote Sens., 35, 321–340, https://doi.org/10.1080/01431161.2013.871083, 2014.

Oliphant, T. E.: A Guide to NumPy, vol. 1, Trelgol Publishing USA, 2006.

Parks, S. A., Miller, C., Parisien, M.-A., Holsinger, L. M., Dobrowski, S. Z., and Abatzoglou, J.: Wildland Fire Deficit and Surplus in the Western United States, 1984–2012, Ecosphere, 6, 1–13, https://doi.org/10.1890/ES15-00294.1, 2015.

Pechony, O. and Shindell, D. T.: Driving Forces of Global Wildfires over the Past Millennium and the Forthcoming Century, Proc. Natl. Acad. Sci., 107, 19 167–19 170, https://doi.org/10.1073/pnas.1003669107, 2010.

Pedregosa, F., Varoquaux, G., Gramfort, A., Michel, V., Thirion, B., Grisel, O., Blondel, M., Prettenhofer, P., Weiss, R., Dubourg, V., Vanderplas, J., Passos, A., Cournapeau, D., Brucher, M., Perrot, M., and Duchesnay, E.: Scikit-Learn: Machine Learning in Python, J. Mach. Learn. Res., 12, 2825–2830, 2011.

Pettinari, M. L. and Chuvieco, E.: Generation of a Global Fuel Data Set Using the Fuel Characteristic Classification System, Biogeosciences, 13, 2061–2076, https://doi.org/10.5194/bg-13-2061-2016, 2016.

https://doi.org/10.5194/bg-2020-409
Preprint. Discussion started: 11 November 2020

Poulter, B., MacBean, N., Hartley, A., Khlystova, I., Arino, O., Betts, R., Bontemps, S., Boettcher, M., Brockmann, C., Defourny, P., Hagemann, S., Herold, M., Kirches, G., Lamarche, C., Lederer, D., Ottlé, C., Peters, M., and Peylin, P.: Plant Functional Type Classification for Earth System Models: Results from the European Space Agency's Land Cover Climate Change Initiative, Geosci. Model Dev., 8, 2315–2328, https://doi.org/10.5194/gmd-8-2315-2015, 2015.

Runge, J., Nowack, P., Kretschmer, M., Flaxman, S., and Sejdinovic, D.: Detecting and Quantifying Causal Associations in Large Nonlinear Time Series Datasets, Sci. Adv., 5, eaau4996, https://doi.org/10.1126/sciadv.aau4996, 2019.

Ryu, Y., Berry, J. A., and Baldocchi, D. D.: What Is Global Photosynthesis? History, Uncertainties and Opportunities, Remote Sensing of Environment, 223, 95–114, https://doi.org/10.1016/j.rse.2019.01.016, 2019.

Sanderson, B. M. and Fisher, R. A.: A Fiery Wake-up Call for Climate Science, Nat. Clim. Chang., 10, 175–177, https://doi.org/10.1038/s41558-020-0707-2, 2020.

Teckentrup, L., Harrison, S. P., Hantson, S., Heil, A., Melton, J. R., Forrest, M., Li, F., Yue, C., Arneth, A., Hickler, T., Sitch, S., and Lasslop, G.: Response of Simulated Burned Area to Historical Changes in Environmental and Anthropogenic Factors: A Comparison of Seven Fire Models, Biogeosciences, 16, 3883–3910, https://doi.org/10.5194/bg-16-3883-2019, 2019.

Teubner, I. E., Forkel, M., Jung, M., Liu, Y. Y., Miralles, D. G., Parinussa, R., van der Schalie, R., Vreugdenhil, M., Schwalm, C. R., Tramontana, G., Camps-Valls, G., and Dorigo, W. A.: Assessing the Relationship between Microwave Vegetation Optical Depth and Gross Primary Production, Int. J. Appl. Earth Obs. Geoinformation, 65, 79–91, https://doi.org/10.1016/j.jag.2017.10.006, 2018.

Thurner, M., Beer, C., Santoro, M., Carvalhais, N., Wutzler, T., Schepaschenko, D., Shvidenko, A., Kompter, E., Ahrens, B., Levick, S. R., and Schmullius, C.: Carbon Stock and Density of Northern Boreal and Temperate Forests, Glob. Ecol. Biogeogr., 23, 297–310, https://doi.org/10.1111/geb.12125, 2014.

Turco, M., Rosa-Cánovas, J. J., Bedia, J., Jerez, S., Montávez, J. P., Llasat, M. C., and Provenzale, A.: Exacerbated Fires in Mediterranean Europe Due to Anthropogenic Warming Projected with Non-Stationary Climate-Fire Models, Nat Commun, 9, 3821, https://doi.org/10.1038/s41467-018-06358-z, 2018.

van Oldenborgh, G. J., Krikken, F., Lewis, S., Leach, N. J., Lehner, F., Saunders, K. R., van Weele, M., Haustein, K., Li, S., Wallom, D., Sparrow, S., Arrighi, J., Singh, R. P., van Aalst, M. K., Philip, S. Y., Vautard, R., and Otto, F. E. L.: Attribution of the Australian Bushfire Risk to Anthropogenic Climate Change, Nat. Hazards Earth Syst. Sci. Discuss., pp. 1–46, https://doi.org/10.5194/nhess-2020-69, 2020.

Van Rossum, G. and Drake, F. L.: Python 3 Reference Manual, CreateSpace, Scotts Valley, CA, 2009.

Virtanen, P., Gommers, R., Oliphant, T. E., Haberland, M., Reddy, T., Cournapeau, D., Burovski, E., Peterson, P., Weckesser, W., Bright, J., van der Walt, S. J., Brett, M., Wilson, J., Jarrod Millman, K., Mayorov, N., Nelson, A. R. J., Jones, E., Kern, R., Larson, E., Carey, C., Polat, İ., Feng, Y., Moore, E. W., Vand erPlas, J., Laxalde, D., Perktold, J., Cimrman, R., Henriksen, I., Quintero, E. A., Harris, C. R., Archibald, A. M., Ribeiro, A. H., Pedregosa, F., van Mulbregt, P., and Contributors, S. . .: SciPy 1.0: Fundamental Algorithms for Scientific Computing in Python, Nat. Methods, https://doi.org/10.1038/s41592-019-0686-2, 2020.

Voulgarakis, A. and Field, R. D.: Fire Influences on Atmospheric Composition, Air Quality and Climate, Curr Pollution Rep, 1, 70–81, https://doi.org/10.1007/s40726-015-0007-z, 2015.

Wagner, W., Lemoine, G., and Rott, H.: A Method for Estimating Soil Moisture from ERS Scatterometer and Soil Data, Remote Sensing of Environment, 70, 191–207, https://doi.org/10.1016/S0034-4257(99)00036-X, 1999.

Westerling, A. L.: Warming and Earlier Spring Increase Western U.S. Forest Wildfire Activity, Science, 313, 940–943, https://doi.org/10.1126/science.1128834, 2006.

https://doi.org/10.5194/bg-2020-409
Preprint. Discussion started: 11 November 2020

Yang, J., Tian, H., Tao, B., Ren, W., Kush, J., Liu, Y., and Wang, Y.: Spatial and Temporal Patterns of Global Burned Area in Response to
550 Anthropogenic and Environmental Factors: Reconstructing Global Fire History for the 20th and Early 21st Centuries, J. Geophys. Res. Biogeosciences, 119, 249–263, https://doi.org/10.1002/2013JG002532, 2014.